

Nonlinear transport in pinned one-dimensional charge-density wave systems*

Marshall J. Cohen and A. J. Heeger

Department of Physics and Laboratory for Research on the Structure of Matter, University of Pennsylvania, Philadelphia, Pennsylvania 19104

(Received 21 March 1977)

The results of an experimental study of nonlinear electrical transport at low temperatures are described for the one-dimensional organic conductors TTF-TCNQ (tetrathiafulvalene-tetracyanoquinodimethane) and TSeF-TCNQ (tetraselenafulvalene-tetracyanoquinodimethane). The b -axis conductivity is nonlinear in both compounds with the onset of nonlinearity at applied electric fields of a few V/cm. Measurements along different crystallographic directions show that the nonlinear transport is directly related to the one-dimensional nature of the electronic system. Traditional single-particle mechanisms of nonlinearity in semiconductors are ruled out through direct experimental study. The experimental results are discussed in terms of nonlinear phase-kink solitons of the pinned charge-density wave condensate at low fields, and field-induced depinning at high fields.

I. INTRODUCTION

In any metal whose Fermi surface contains macroscopic nested sections, a periodic lattice distortion (PLD) will arise whose periodicity results in the opening of a small (compared to the bandwidth) gap in the electronic energy spectrum at the Fermi surface. The PLD is accompanied by a periodic distortion in the conduction-electron charge density; a charge-density wave (CDW). In a one-dimensional metal, the Fermi surface is perfectly nested, implying a PLD with wave number $q_0 = 2k_F$.¹

In a single-particle semiconductor, the gap results from the periodic perturbing effects of the equilibrium ionic lattice and is thus necessarily tied to the lattice. The Peierls gap, however, results from the PLD and is thus tied only to the distortion and not necessarily to the lattice itself.² If the PLD is commensurate with the lattice, it corresponds to a standing wave, and the Peierls state is semiconducting. If the PLD is incommensurate with the lattice, it is possible to visualize excited states where the phase of the PLD moves through the crystal carrying the CDW. In this case, the Peierls state is conducting in a collective many-body sense as first described by Fröhlich.²

TTF-TCNQ (tetrathiafulvalene-tetracyanoquinodimethane) crystallizes in regular segregated stacks of TCNQ acceptors and TTF donors.³ Experimental studies of dc electrical conductivity,⁴⁻⁷ microwave transport,⁸⁻¹⁰ and optical reflectance¹¹⁻¹⁴ have clearly established the one-dimensional (1D) properties of TTF-TCNQ in the metallic state. From the earliest data, it was suggested that the behavior of TTF-TCNQ was associated with the Peierls instability.⁴

The structural studies¹⁵⁻²² have now established that TTF-TCNQ undergoes a sequence of three successive phase transitions at 54, 49, and 38 K

respectively, from a 1D conductor above 54 K to a high-dielectric-constant anisotropic semiconductor below 38 K. The low-temperature phase is characterized by a PLD and an associated CDW ground state.

Above 54 K diffuse x-ray-scattering experiments^{15, 16, 18, 21, 22} have shown that the coupled conduction-electron-lattice system fluctuates into an incommensurate CDW which increases in amplitude as the temperature is lowered, but with phase which is arbitrary with respect to the undistorted lattice. In an ideal system, the fluctuating CDW can move to form a current carrying state.² In a real system, impurities and defects lead to pinning effects and thus resistive fluctuations.²³ Experimentally, at high temperatures, the dominant fluctuations appear to be current carrying and the resistive fluctuations dominate only in a relatively narrow temperature range just above the 54-K transition where the interchain phase relation is set²² (i.e., the growth of transverse coherence between CDW's on neighboring chains). The conductivity thus increases as the temperature is lowered from room temperature to 58 K and decreases rapidly⁴ between 58 K and the first transition at 54 K.

At the structural transitions, both the PLD and the CDW are pinned to the equilibrium lattice. The simplest mechanism for the propagation of current is the independent particle excitation of electron-hole pairs across the semiconductor (Peierls) gap. The activation energy would scale with the width of the Peierls gap, and the magnitude of the conductivity would involve the single-particle mobility and the total conduction-electron oscillator strength.

If the forces which pin the CDW's to the equilibrium lattice are sufficiently small, it may be possible for segments to become depinned thermally and their phases put in motion with the application of a

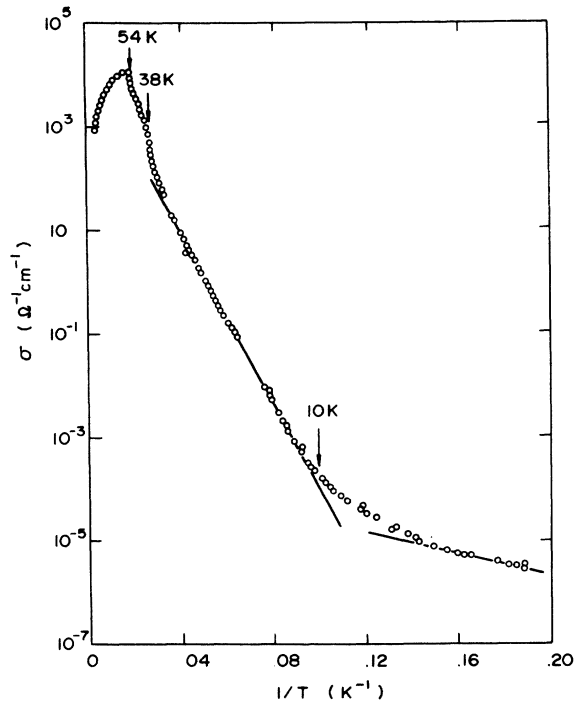


FIG. 1. dc conductivity of TTF-TCNQ between 5 and 300 K. The anomalies in the conductivity which appear at the structural phase transitions near 54 and 38 K are indicated (see text).

field.^{23(a)} It has also been suggested²⁴ that if the pinned CDW's are compressible, an excited state would consist of mobile charge-carrying compressions and rarefactions which would be conductive.

Figure 1 shows the temperature-dependent conductivity of TTF-TCNQ in the chain direction plotted as $\ln\sigma$ vs $1/T$. As can be seen, below ~ 40 K, the conductivity can be characterized by two activated processes. The high-temperature ($40 > T > 20$ K) process has both a larger activation energy and a larger magnitude and is due to the thermal activation of electron-hole pairs across the Peierls gap. The low-temperature ($T \leq 10$ K) process is the subject of this paper.

II. EXPERIMENTAL TECHNIQUES

The experiments described in this paper consist of measurements of the current-voltage characteristics of high-purity single crystals of TTF-TCNQ and the selenium analog salt TSeF-TCNQ.²⁵ The measurements were carried out using both dc and pulsed techniques. As the sample resistance tended to exceed $10^9 \Omega$, special precautions were taken to avoid loading the measurement apparatus. All dc measurements were carried out on single crystals using the standard four-probe arrangements with the sample immersed in a liquid-helium bath.

Currents were supplied with a simple dividing network using a battery source and were measured with an ammeter floated from the lab ground. Voltages were measured using an electrometer as a gain-of-one impedance buffer between the sample and a digital multimeter.

To avoid heating the samples, measurements at higher current densities were carried out using pulsed techniques. Again precautions were necessary to avoid reflections from the sample cable [Fig. 2(a)]. The dc supply was used to bias the sample to a point where its dynamic impedance was less than about $5 M\Omega$. The $50\text{-}\Omega$ resistor matched the output impedance of the pulse generator near the sample and the capacitor isolated the dc bias from the pulse generator.

The resistance of crystals of TSeF-TCNQ in the liquid helium range tends to be of order $10^3 \Omega$ or less, so four-probe pulsed techniques shown in Fig. 2(b) were possible.

III. EXPERIMENTAL RESULTS

Figure 3 shows the current-voltage characteristics of a single crystal of TTF-TCNQ measured along the principle conducting \vec{b} direction over the temperature range between 1.6 and 4.2 K. The data shown were obtained using the dc technique described above, and the upper limit of $1 \mu A$ was chosen to avoid heating the sample. At the lowest fields, corresponding to voltages less than about 0.2 V, the data are Ohmic and the conductivity decreases

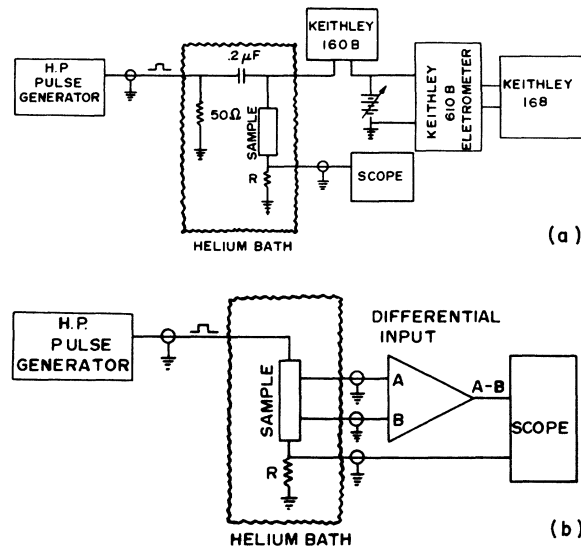


FIG. 2. Circuitry used during pulsed I - V measurements. High-impedance samples were measured with a two-probe circuit (a) while under dc bias and low-impedance samples were measured with a four-probe circuit (b).

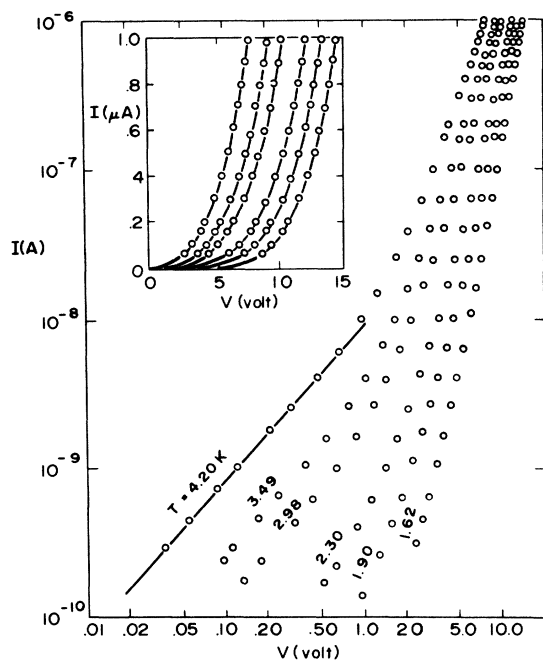


FIG. 3. dc current-voltage characteristics of single crystals of TTF-TCNQ measured along the \vec{b} axis at temperatures between 1.6 and 4.2 K.

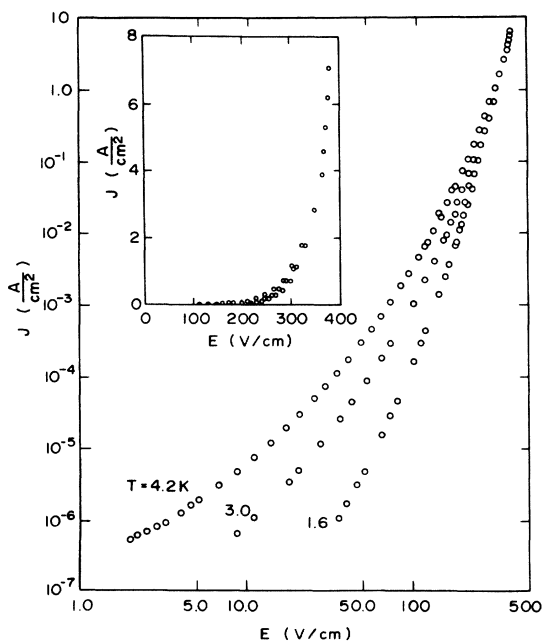


FIG. 4. j vs E for TTF-TCNQ covering the range $10^{-6} < j < 10$ A/cm². dc techniques were used for $j < 5 \times 10^{-2}$ A/cm²; pulsed measurements covered the range above 10^{-2} A/cm².

exponentially as the temperature is lowered. As the electric field is increased, the data become non-Ohmic with the dynamic conductance, dI/dV increasing with increasing field. The degree of nonlinearity as indicated in the full logarithmic plot increases dramatically as the temperature is lowered with the result that the curves appear to be converging at some characteristic electric field. The degree of nonlinearity can be clearly seen in the linear plot in the inset.

To examine this effect more carefully, the measurements were extended to higher current densities using the high-impedance pulsed techniques. Figure 4 shows the results at three temperatures. The data are plotted as current density versus electric field; the various temperature curves converge near a field of 400 V/cm. The inset displays the same data plotted linearly. The I - V curves qualitatively appear to be approaching an off-on situation at absolute zero where current is not generated until a critical electric field is reached.

It is natural to question whether the observed nonlinearities in the I - V characteristics of TTF-TCNQ are related to its one dimensionality. To this end, we have measured the I - V characteristics of single crystals of TTF-TCNQ whose needle axis was oriented along the crystallographic \vec{a} axis, the direction of alternating stacks of TTF and TCNQ molecules. Figure 5 shows the normalized field-

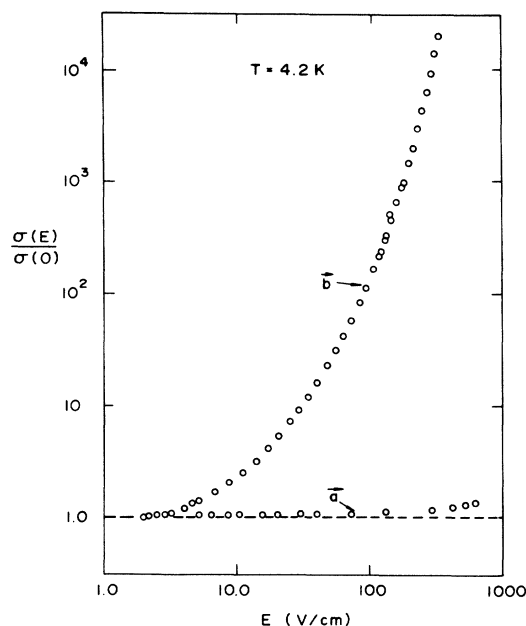


FIG. 5. Normalized field-dependent conductivity $\sigma(E) \equiv j(E)/E$ of TTF-TCNQ measured along the principal conductivity \vec{b} axis and the transverse \vec{a} axis at 4.2 K.

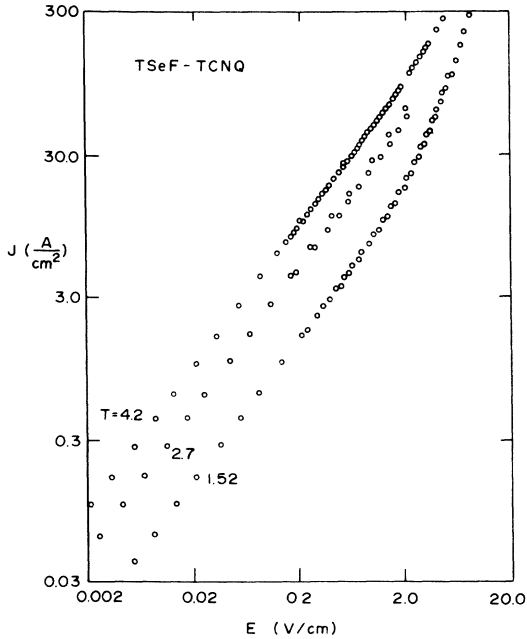


FIG. 6. j vs E for single crystals of TSeF-TCNQ measured along the \vec{b} axis. The data represent a composite of dc and pulsed measurements.

dependent conductivity $\sigma(E) = J/E$ plotted versus electric field for both \vec{b} and \vec{a} directions. The conductivity along \vec{b} increases by more than 10^4 over the range of electric field where the \vec{a} -axis conductivity is Ohmic. The conductivity along \vec{c} was too small to provide measurable currents at applied fields of less than 10^3 V/cm so we were unable to repeat the measurements in that direction.

Figure 6 shows a combination of dc and pulsed I - V measurements we performed on the isostructural salt TSeF-TCNQ in which all four sulfurs on the TTF molecules are replaced with selenium. The Ohmic conductivity at 1.5 K is more than seven orders of magnitude greater than that of TTF-TCNQ. Nevertheless, the TSeF-TCNQ conductivity becomes nonlinear at approximately the same electric field. Due to the large absolute magnitude of σ for TSeF-TCNQ even at low temperatures, measurements at higher electric fields than those shown were impossible due to sample heating.

IV. DISCUSSION OF RESULTS

Whenever non-Ohmic conductivity is observed, care must be taken to ascertain that the data are intrinsic to the material and do not arise from the measurement technique. This is especially true with a semiconducting sample, i.e., one whose resistivity has a negative temperature coefficient. The two major sources of extrinsic nonlinearities are the injection of charge at a non-Ohmic (recti-

fying) contact and the joule heating of the sample to a higher temperature and thus lower-resistivity state.

It is often difficult to make contact to a nonmetallic sample due to non-Ohmic (and potentially nonlinear) contact resistance. Equipotential-mapping experiments on TTF-TCNQ have revealed the existence of contact resistance at the silver paint-sample interface.²⁶ We have performed voltage-dependent contact-resistance measurements at higher temperatures and found these contacts to be Ohmic.⁴ This type of verification is impossible at low temperatures where the sample resistance is believed to be intrinsically nonlinear. When the four-probe measurement configuration is used, possible rectification at the current contacts is not important as the actual current that enters the sample is measured directly. The electrometer, however, measures the voltage drop by drawing current through the voltage contacts. The observed nonlinearity may simply be due to rectifying properties of the voltage contacts. As the input impedance of the electrometer is greater than 10^{14} Ω , and the sample resistance is less than 10^9 Ω in the nonlinear regime, less than one part in 10^5 of the applied current is drawn through the voltage contacts.

The measurements were repeated in a two-probe configuration using the voltage leads and the results were identical to the four-probe measurements. In this configuration, all of the current is drawn through the voltage contacts. Since a factor of 10^5 change in the current passing through the voltage contacts caused no change in the I - V characteristics, we can conclude that the observed data do not result from contact rectification and that any contact resistance is negligible compared to the sample resistance.

If a non-Ohmic current contact is applied to an insulating sample, it is possible to inject carriers which would drift through the sample in a manner analogous to leakage current in a capacitor.²⁷ Due to the extremely high dielectric constant of TTF-TCNQ at low temperatures; greater than 3000, the sample may be considered a parallel plate capacitor filled with a dielectric medium. The leakage current density is given by $j = (Q/A)/\tau$, where τ is the transit time which can be reexpressed in terms of the drift mobility μ the electric field E , and the length of the sample, d . When the charge (Q) is reexpressed in terms of the capacitance of the contacts and dielectric constant of the sample, the result is

$$j = (\epsilon \mu / d) E^2.$$

The current density thus depends quadratically on the electric field and a mobility can be inferred from measurements of j and E . The data of Figs.

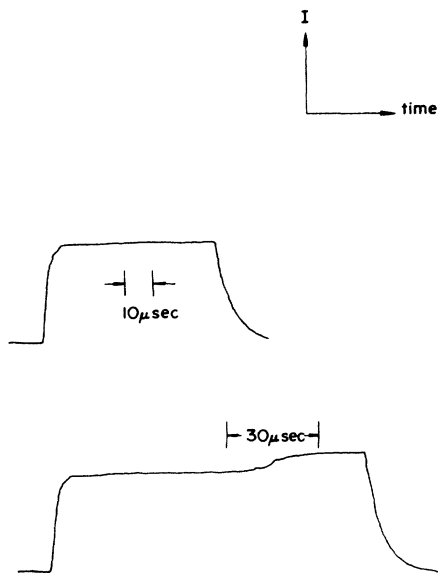


FIG. 7. Effect of sample heating at current densities greater than 10 A/cm^2 on the current measured during pulsed I - V measurements (see text). The two pulses differ only in duration. Sample heating is evident after approximately $60 \mu\text{sec}$.

3 and 4 imply a mobility greater than $10^4 \text{ cm}^2/\text{Vsec}$, a value three to four orders of magnitude greater than found in even the purest single-crystal organic semiconductors.²⁷

A second source of nonlinearity in a semiconducting sample comes from self-heating. The magnitude of this effect can be estimated using the thermal time constant observed during specific-heat measurements.²⁸ The relaxation time is related to the specific heat by the expression $[\tau_{\text{th}} = Nc/K(A/l)]$, where N is the number of moles of material with specific heat c and thermal conductance K , and A and l are the area and length respectively. If we assume that the outside of the sample is in thermal equilibrium with the helium bath, then the temperature gradient between the center and surface of the sample is related to its thermal conductivity and the power input. The I - V data are highly nonlinear at input powers of less than 10^{-10} W implying a temperature gradient of less than a millidegree which is negligible compared to the nonlinearities observed.

A more direct observation of the effects of heating was obtained during the pulsed I - V measurements. The measurement was made with a constant pulsed voltage across the sample and current resistor. As the sample heated, its resistance decreased causing more current to flow through the resistor. This effect is shown in Fig. 7 which is an actual trace of the current pulse captured

with a wave-form recorder. The two traces differ only in the length of the pulse. For pulse widths less than about $20 \mu\text{sec}$, heating was unimportant. The thermal time constant for this sample is about $30 \mu\text{sec}$ so the sample completely cooled during the tenth of a second between pulses. The ability to observe heating directly allows us to have the confidence that all the data shown are intrinsic to the sample.

Intrinsic nonlinearities which are unrelated to the CDW ground state of TTF-TCNQ must also be considered. The two most common single-particle mechanisms are field ionization and impact ionization of charged impurities.

Bound impurities in a semiconductor can be viewed as being separated from the conduction band by a potential barrier. The tunneling probability for a bound electron to ionize can become significant if the electric field energy over the localization length of the impurity can compete with the available thermal energy. Otherwise, any bound electron that could possibly have tunneled to the conduction band has already been thermally ionized, and thus no new carriers would be created by the electric field. To ionize impurity electrons with a binding energy of order 20 K with an electric field of about 100 V/cm would require that the impurity wave function extend over lengths of order 10^3 \AA .

It is possible, however, to generate extra carriers with low-level electric fields if free electrons can be accelerated to sufficient kinetic energies to ionize bound electrons upon collision.³⁰ This depends directly on the mobility of the crystal and would require $\mu \geq 10^5 \text{ cm}^2/\text{V sec}$ at the fields observed.

The possibility of impact ionization was studied experimentally with radiation-damage measurements. Single crystals of TTF-TCNQ were bombarded with 8-MeV deuterons and the resultant electrical properties were measured. The temperature dependent I - V curves shown in Fig. 8 were obtained from a crystal irradiated with a flux of $5 \times 10^{14} \text{ cm}^{-2}$ which increased the room temperature resistance by 10% . The figure also shows prebombardment data for comparison. The irradiation has induced charged defects which increased the Ohmic conductivity at 4.2 K by more than two orders of magnitude. The defect contribution to the conductivity is ohmic and activated with an energy of 20 K . The previously observed nonlinearity is masked at 4.2 K by the larger defect contribution. At 1.5 K , where the defect conductivity is small and unimportant, the nonlinearity shows up clearly with identical curvature as a function of applied voltage. Preliminary ESR measurements estimate the defect concentration to be of order a tenth of a percent, a value which would certainly decrease the

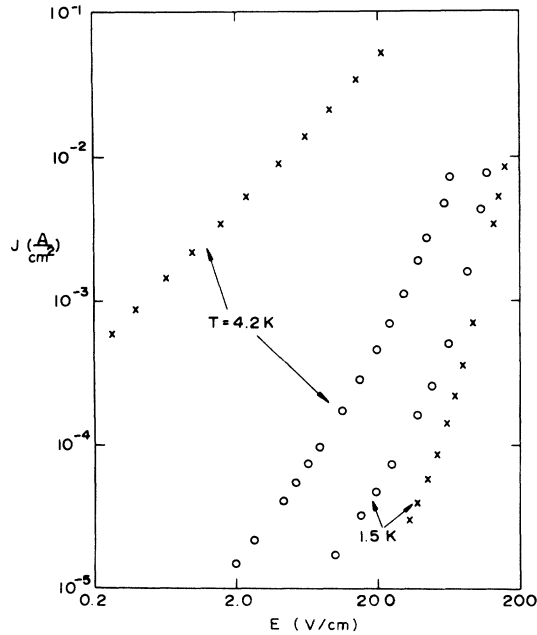


FIG. 8. j vs E for TTF-TCNQ measured along the \vec{b} axis before (○○○) and after (×××) irradiation with deuterons (see text).

mobility of the crystal. The invariance of the nonlinearities after bombardment is a clear indication that they do not arise from impact ionization.

In Fig. 9, we have plotted the data as the log of current versus inverse temperature at fixed values of the electric field. The general features are those of a thermally activated conductivity with the activation energy decreasing with increasing electric field. The field-dependent activation energy as obtained from the slopes of the curves is plotted in the inset which shows Δ decreasing approximately linearly with increasing field and extrapolating to zero at a field of about 125 V/cm. For fields less than that, the data are adequately described by the expression

$$j/E = \sigma_0 \exp[-(\Delta/T)(1 - E/E_0)].$$

The characteristic field obtained from several samples is 150 ± 50 V/cm and the conductivity prefactor σ_0 ranges between 5×10^{-5} and 3×10^{-4} with 10^{-4} ($\Omega \text{ cm}$) $^{-1}$ being a typical value. The sample dependence of the characteristic field is consistent with the errors involved in determining the distance between voltage contacts on small samples. The zero-field activation energy is approximately 14 K with a sample dependence of only about a degree. At fields less than the characteristic field E_0 the prefactor σ_0 is only weakly field dependent with σ_0 increasing by less than a factor of two over a range where J/E changes by three orders of mag-

nitude at the lowest temperatures. At higher fields the activation energy no longer decreases but saturates at a small value (about 4 K in this sample), but σ_0 begins to increase exponentially with field. The 1.6-K data (Fig. 4) represent a total increase in conductivity of six orders of magnitude from 3×10^{-8} at $E = 30$ V/cm to $2 \times 10^{-2} \Omega^{-1} \text{ cm}^{-1}$ at 380 V/cm.

V. CONDUCTIVITY OF THE PINNED CDW SYSTEM

The data presented above can be qualitatively described in terms of the pinned CDW ground state of TTF-TCNQ. The pinning potential is necessarily periodic and the simplest form²⁴ is

$$V = V_0(1 - \cos \phi)$$

If the pinning were to arise from the Coulomb interactions between charge-density waves on neighboring chains, the periodicity of the potential would be the same as that of the charge-density wave, i.e., $\phi = (2\pi/\lambda_s)X$ where $\lambda_s = 3.4b$.¹⁵⁻²² If the pinning were to arise from the commensurability of the charge-density wave with the equilibrium lattice, the periodicity would be that of the lattice, i.e., $\phi = (2\pi/b)X$. The magnitude of the pinning potential can be estimated by expanding the poten-

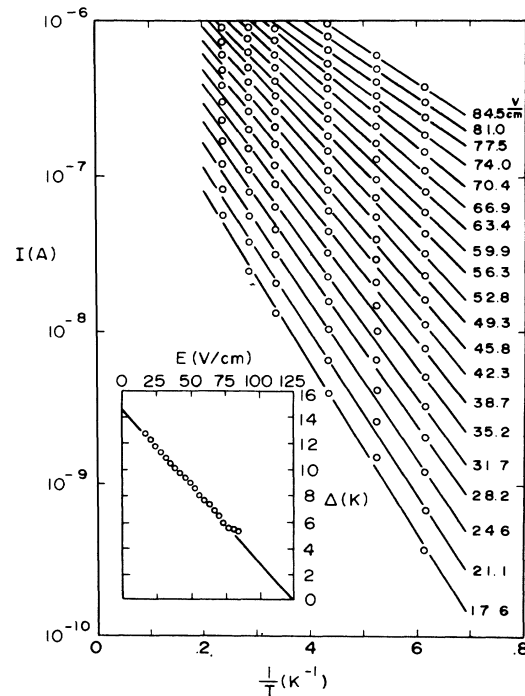


FIG. 9. Data of Fig. 3 replotted as $\ln I$ vs T^{-1} at various values of the applied electric field. The solid lines represent least-squares fits to the data at each field. The field-dependent activation energy is shown in the inset.

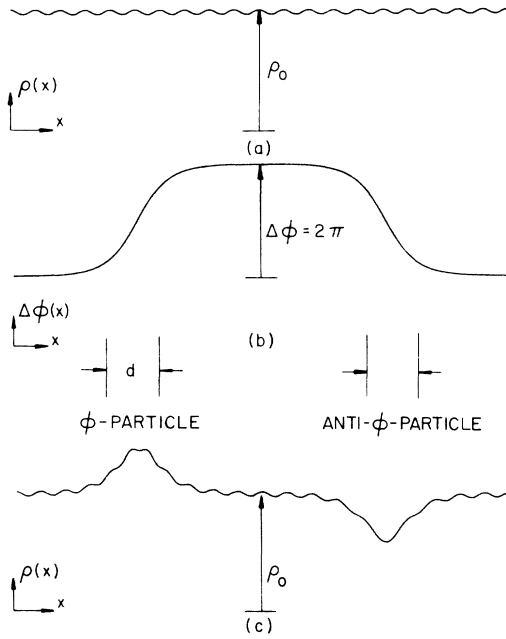


FIG. 10. (a) Rigid charge density wave; $\rho = \rho_0 + \rho_1 \cos(2k_F x)$, where $\rho_1/\rho_0 \approx 0.02$. (b) Phase kinks of $\pm 2\pi$ as described by Eq. (5). (c) Charge density in presence of phase kinks

$$\rho = \rho_0 + \rho_1 \cos[2k_F x + \phi(x)] + \frac{N_s e}{2k_F} \frac{d\phi(x)}{dx},$$

where $\phi(x)$ is shown in (b).

tial and comparing the quadratic term with the pinning frequency determined by far-infrared reflectance measurements

$$V_0 (2\pi/\lambda)^2 = M_F^* \omega_F^2. \quad (2)$$

$\lambda = b$ (commensurability pinning) or $\lambda = 3.4b$ (Coulomb pinning). A Fröhlich effective mass³⁰ of $M_F^* \approx 1400m^*$ (m^* is the single-particle band mass) and a pinning frequency³⁰ of $\omega_F \approx 2 \text{ cm}^{-1}$ corresponds to a pinning potential energy of $eV_0 \approx 17 \text{ K}$ (commensurability pinning) or 1.5 K (Coulomb pinning).

The current carried by a charge-density wave system depends on the coherent motion of its phase with respect to the stationary lattice.³¹ The full Lagrangian density of the CDW system must include a potential energy due to its compressibility. This has been found by Rice *et al.*²⁴ to be

$$U_{\text{comp.}} = \frac{1}{2} N_s M_F^* (c_0/q^*)^2 [\nabla_x \phi(x)]^2 \quad (3)$$

where N_s is the 1D density of condensed electrons, $q^* = 2\pi/\lambda_s$ and c_0 is the characteristic phase velocity given by $c_0 = v_F (m^*/m_F^*)^{1/2}$. The equation of motion²⁴ with the phase as the generalized coordinate is:

$$\ddot{\phi} - c_0^2 \nabla_x^2 \phi + \omega_F^2 \frac{dV}{d\phi} = 0. \quad (4)$$

If the pinning potential of Eq. (1) is used, this is the sine-Gordon equation for which there exists a class of exact nonlinear solitary wave solutions given by^{24,32}

$$\phi_{\pm}(X - vt) = 4 \tan^{-1} \left\{ \exp \pm \left[\frac{\omega_F}{c_0} \frac{X - vt}{(1 - v^2/c_0^2)^{1/2}} \right] \right\}. \quad (5)$$

These correspond to phase "kinks" of $\pm 2\pi$ localized over a length $d \sim c_0/\omega_F (1 - v^2/c_0^2)^{1/2}$ and propagating with a velocity v . For TTF-TCNQ $d(v=0) \sim 20b \sim 6\lambda_s$. The phase kinks are illustrated in Fig. 10(b). Figure 10(c) shows the periodic charge density as a function of $\phi(x)$ with the result that the phase kinks correspond to mobile localized charges.

The Lagrangian density can be converted into a Hamiltonian density and the solutions of Eq. (4) result in an energy spectrum given by²⁴

$$E(v) = \frac{M_{\phi} c_0^2}{(1 - v^2/c_0^2)^{1/2}}, \quad (6)$$

where the energy has been expressed in terms of a "rest mass":

$$M_{\phi} = 8N_s M_F^* / q^{*2} d. \quad (7)$$

The phase kinks can thus be thought of as charged quasiparticles with mass M_{ϕ} and rest energy $M_{\phi} c_0^2$. In the absence of a driving force, these " ϕ -particles" are thermally excited with an activation energy of order the rest energy.

For TTF-TCNQ, the ϕ -particle rest mass as estimated from Eq. (7) is about 12 K (commensurability pinning) or 140 K (Coulomb pinning). The measured zero-field activation energy of 14 K is in close agreement with the former. Similar measurements on TSeF-TCNQ found an activation energy of about 5 K. The conductivity due to ϕ particles can be written²⁵

$$\sigma_0 = \sigma_0(T) e^{-\Delta/T} = \mu_{\phi} e^* N_{\phi} e^{-M_{\phi} c_0^2/T}, \quad (8)$$

$$N_{\phi} \sim (b/d) N_s, \quad \mu_{\phi} = eV_{\text{th}} b/k_B T.$$

We have assumed that the density of ϕ particles scales with the density of condensed conduction electrons and that the mobility was thermally diffusive. The diffusion constant is a thermal velocity given by $\frac{1}{2} m v_{\text{th}}^2 = k_B T$ times a characteristic length which we assume to be a lattice constant. At 1.5 K, Eq. (8) gives $\mu_{\phi} \sim 10 \text{ cm}^2/\text{V sec}$. Using the expression above for the density of particles, the conductivity prefactor of TTF-TCNQ and TSeF-

TCNQ can be used to imply a mobility. The conductivity prefactor of TSeF-TCNQ is of order $10^2 \Omega^{-1} \text{cm}^{-1}$ which implies a mobility of about $10 \text{ cm}^2/\text{V sec}$ in agreement with the calculated value. On the other hand, the conductivity prefactor of TTF-TCNQ is six orders of magnitude lower implying a mobility of only $10^{-5} \text{ cm}^2/\text{V sec}$.

The phase kinks described earlier are solutions of the equation of motion [Eq. (4)] only in the absence of a driving force. Qualitatively as the electric field is increased the effective pinning potential is decreased; thus an electric field would have the effect of lowering the ϕ -particle activation energy. The low-temperature CDW conductivity can thus be pictured as being characterized by two values of the electric field. At the lowest fields the nonlinearity is determined by the field (E_0) required to reduce the ϕ -particle activation energy to zero. This is of order 150 V/cm as discussed above. The upper characteristic electric field (E_1) is that which is sufficient to reduce the magnitude of the potential to zero; $(\lambda_s/2\pi)E_1 = V_0$. For interchain Coulomb pinning, the upper (E_1) field is of order 10^3 V/cm . Above this upper field, the conductivity would again be Ohmic as the entire CDW system is depinned.

The order of magnitude of the conductivity of the depinned CDW system can be estimated from the oscillator strength and lifetime as determined from the far-ir experiments³⁰ to be of order $10^2 (\Omega \text{ cm})^{-1}$. For TSeF-TCNQ, $\sigma_{\text{max}} \approx 30 (\Omega \text{ cm})^{-1}$ at 1.5 K implying that the CDW system is nearly completely depinned at $E \sim 10 \text{ V/cm}$. For TTF-TCNQ, $\sigma_{\text{max}} \approx 2 \times 10^{-2} (\Omega \text{ cm})^{-1}$ at 400 V/cm . In both cases, sample heating restricts the measurements to fields below E_1 .

VI. SUMMARY AND CONCLUSION

We have presented an experimental study of nonlinear electrical transport phenomena at low temperatures in the 1D organic conductors TTF-TCNQ and TSeF-TCNQ. The principle experimental results are as follows:

- (i) The b -axis conductivity is nonlinear in both compounds. Although the absolute values of the low-field conductivities differ by nearly six orders of magnitude, both compounds show the onset of nonlinearity with applied electric fields of a few V/cm (Figs. 3, 4, and 6).
- (ii) The nonlinear transport is directly related to the 1D nature of the electronic system. The b -axis conductivity increases by nearly five orders of magnitude in a range of electric fields where the a -axis conductivity is constant (Fig. 5).
- (iii) Traditional single particle mechanisms of I - V nonlinearity in semiconductors have been

checked through direct experimental studies. In particular, the onset of sample heating is clearly identified in the pulsed field studies (Fig. 7). At lower levels the observed nonlinearity results directly from nonlinear conduction in the electronic system. High mobility mechanisms are ruled out by the insensitivity of the nonlinearity to radiation induced defects (Fig. 8).

The experimental results were discussed in terms of the nonlinear phase-kink-soliton excitations of the pinned CDW system. Although the structural studies have provided detailed evidence of the pinned CDW ground state, the excitations will depend on the nature and origin of the pinning potential $V(\phi)$. In this paper, we have assumed $V(\phi)$ to be of the simple sinusoidal form thus leading naturally to the sine-Gordon equation and ϕ -particle excitations. A general property of this kind of system, characterized by an anharmonic potential plus dispersion, is the existence of two classes of solutions; small amplitude harmonic solutions (in the CDW case these are the phason modes of Lee, Rice, and Anderson),³³ and large amplitude nonlinear kink solutions (the ϕ particles of Rice, Bishop, Krumhansl, and Trullinger).²⁴ There is ample experimental evidence in the pinned CDW systems for the small amplitude solutions. In particular, the unusually large dielectric constants ($\epsilon_1 = 3500$ for^{8,18,34} TTF-TCNQ and $\epsilon_1 = 16000$ for³⁴ TSeF-TCNQ in the presence of a relatively large energy gap indicate low-frequency oscillator strength consistent with the small amplitude excitations.

To our knowledge, at present the only evidence relevant to the proposed phase-kink excitations comes from the nonlinear transport data. The rest mass energies and characteristic electric fields inferred from the data are in reasonable agreement with theoretical estimates. The absolute magnitude of the high-field conductivity and the low-field mobility present a more serious puzzle. For TTF-TCNQ, the values are approximately four to five orders of magnitude too small (even though j/E has increased by more than six orders of magnitude in the experimental range studied). For TSeF-TCNQ, both the low-field mobility and high-field conductivity are in good agreement with the magnitudes expected for ϕ -particle diffusive transport (at low fields) and the nearly complete depinned CDW transport (at high fields). The problem may in part arise from the experimental limitations; the TTF-TCNQ curve at 1.5 K is so steep (see Fig. 4) that a 10% increase in applied electric field would bring the absolute magnitude up to the fully depinned value. Unfortunately, this higher current regime brings the power level up to such high values that heating effects are unavoidable even with pulsed techniques.

In conclusion, the results presented in this paper provide indirect evidence of transport by collective excitations of the pinned CDW system. Verification of the proposed charged ϕ -particle excitations in pinned CDW condensates will require further experiments which are more directly sensitive to the presence of such excitations.

ACKNOWLEDGMENTS

We thank Dr. Paul R. Newman for extensive help in the early phases of this work, and for many important discussions on various aspects of the experimental results. We are grateful to Professor

J. Krumhansl, Dr. M. J. Rice, Dr. A. Bishop, and Dr. S. Trullinger for important discussions and considerable encouragement. Dr. M. J. Rice generously supplied us with his lecture notes on various aspects of the pinned CDW and the phase-soliton problem. The irradiation experiments could not have been done without the help of Professor R. Zurmuhle and L. Mulligan. We thank William Gunning, Dr. L. Scott Smith, and Fred Klinker for help on several aspects of the problem. The high-quality crystals used in this study were grown at the University of Pennsylvania by Paul Nigrey.

*Work supported by the NSF through Grant No. DMR-76-2-1667. The synthesis, purification, and crystal growth which made these studies possible were supported by the NSF Materials Research Laboratory at the University of Pennsylvania, DMR-76-00678.

¹R. E. Peierls, *Quantum Theory of Solids* (Oxford U.P., London, England, 1955), p. 108.

²H. Fröhlich, Proc. R. Soc. A 223, 296 (1954); J. Bardeen, Solid State Commun. 13, 357 (1973); D. Allender, J. W. Bray, and J. Bardeen, Phys. Rev. B 9, 119 (1974).

³T. J. Kistenmacher, T. E. Phillips and D. O. Cowan, Acta Crystallogr. B 30, 763 (1974); R. H. Blessing and P. Coppens, Solid State Commun. 15, 215 (1974); A. J. Schultz, G. D. Stucky, R. H. Blessing and P. Coppens, J. Am. Chem. Soc. 98, 3194 (1976).

⁴L. B. Coleman, M. J. Cohen, D. J. Sandman, F. G. Yamagishi, A. F. Garito, and A. J. Heeger, Solid State Commun. 12, 1125 (1973); M. J. Cohen, L. B. Coleman, A. F. Garito, and A. J. Heeger, Phys. Rev. B 10, 1298 (1974).

⁵J. P. Ferraris, D. O. Cowan, V. V. Walatka, and J. H. Perlstein, J. Am. Chem. Soc. 95, 948 (1973).

⁶R. Groff, A. Suna, and R. Merrifield, Phys. Rev. Lett. 33, 418 (1974).

⁷R. J. Warmack, T. A. Callcott, and H. C. Schweinler, Appl. Phys. Lett. 24, 635 (1974).

⁸S. K. Khanna, E. Ehrenfreund, A. F. Garito, and A. J. Heeger, Phys. Rev. B 10, 2205 (1974).

⁹S. K. Khanna, A. F. Garito, A. J. Heeger, and R. C. Jaklevic, Solid State Commun. 16, 667 (1975).

¹⁰M. Cohen, S. K. Khanna, W. J. Gunning, A. F. Garito, and A. J. Heeger, Solid State Commun. 17, 367 (1975).

¹¹A. A. Bright, A. F. Garito, and A. J. Heeger, Solid State Commun. 13, 943 (1973); Phys. Rev. B 10, 1328 (1974).

¹²P. M. Grant, R. L. Greene, G. C. Wrighton, and G. Castro, Phys. Rev. Lett. 31, 1311 (1973).

¹³D. B. Tanner, C. S. Jacobsen, A. F. Garito, and A. J. Heeger, Phys. Rev. Lett. 32, 1301 (1974); Phys. Rev. B 13, 3381 (1976).

¹⁴C. S. Jacobsen, D. B. Tanner, A. F. Garito, and A. J. Heeger, Phys. Rev. Lett. 33, 1559 (1973).

¹⁵F. Denoyer, R. Comès, A. F. Garito, and A. J. Heeger, Phys. Rev. Lett. 35, 445 (1975).

¹⁶S. Kagoshima, H. Anzai, K. Kajimura, and T. Ishiguro, J. Phys. Soc. Jpn. 39, 1143 (1975).

¹⁷R. Comès, S. M. Shapiro, G. Shirane, A. F. Garito, and A. J. Heeger, Phys. Rev. Lett. 35, 1518 (1975); R. Comès, S. M. Shapiro, G. Shirane, A. F. Garito, and A. J. Heeger, Phys. Rev. B 14, 2376 (1976).

¹⁸S. Kagoshima, T. Ishiguro, and H. Anzai, J. Phys. Soc. Jpn. 41, 2061 (1976).

¹⁹H. A. Mook and C. R. Watson, Phys. Rev. Lett. 36, 801 (1976).

²⁰G. Shirane, S. M. Shapiro, R. Comès, A. F. Garito, and A. J. Heeger, Phys. Rev. B 14, 2325 (1976); W. D. Ellenson, R. Comès, S. M. Shapiro, G. Shirane, A. F. Garito, and A. J. Heeger, Solid State Commun. 20, 53 (1976).

²¹J. P. Pouget, S. K. Khanna, F. Denoyer, R. Comès, A. F. Garito, and A. J. Heeger, Phys. Rev. Lett. 37, 437 (1976).

²²S. K. Khanna, J. P. Pouget, R. Comès, A. F. Garito, and A. J. Heeger (unpublished).

²³H. Fukayama, T. M. Rice, and C. M. Varma, Phys. Rev. Lett. 33, 305 (1974); (a) L. Pietronero, S. Strässler, and G. A. Toombs, Phys. Rev. B 12, 5213 (1975).

²⁴M. J. Rice, A. R. Bishop, J. A. Krumhansl, and S. E. Trullinger, Phys. Rev. Lett. 36, 432 (1976).

²⁵S. Etemad, T. Penney, E. M. Engler, B. A. Scott, and P. E. Seiden, Phys. Rev. Lett. 34, 741 (1975).

²⁶L. R. Bickford and K. K. Kanazawa, J. Phys. Chem. Solids 37, 839 (1976).

²⁷F. Gutmann and L. E. Lyons, *Organic Semiconductors* (Wiley, New York, 1967).

²⁸T. Wei, S. Etemad, A. F. Garito, and A. J. Heeger, Phys. Lett. A 45, 269 (1973); and T. Wei (private communication).

²⁹N. Sklar and E. Bursten, J. Phys. Chem. Solids 2, 1 (1957).

³⁰L. B. Coleman, C. R. Fincher, Jr., A. F. Garito, and A. J. Heeger, Phys. Status Solidi B 75, 239 (1976).

³¹M. J. Rice, in *Low-Dimensional Cooperative Phenomena*, edited by H. J. Keller (Plenum, New York, 1975), p. 23.

³²G. B. Whitham, *Linear and Nonlinear Waves* (Wiley, New York, 1974).

³³P. A. Lee, T. M. Rice and P. W. Anderson, Solid State Commun. 14, 703 (1974).

³⁴W. J. Gunning, S. K. Khanna, A. F. Garito, and A. J. Heeger, Solid State Commun. 21, 6 (1977).